JOURNAL OF MATERIALS SCIENCE 28 (1993) 2733–2737

Solidification of undercooled Ni–32.5 wt % Sn eutectic alloy

L.Q. XING*, D.Q. ZHAO, X.C. CHEN
Institute of Physics, Academia Sinica, Beijing, 100 080, People's Republic of China

Bulk Ni–32.5 wt% Sn alloy was undercooled by purification. The solidification characteristics at different undercoolings and the various microstructures were studied. It was found that the two eutectic phases can grow in a matching form, to produce regular eutectic structures if the melt was undercooled by less than 10 K. If the melt was highly undercooled, the dendrite tip velocity of the Ni_3Sn phase was very much larger than that of Ni(α) phase during recalescence; as a result, the melt did not solidify in the regular eutectic morphology but in the dendrite cluster morphology with Ni_3Sn phase acting as the leading phase in the recalescence stage. The dendrite clusters subsequently developed into anomalous eutectic microstructures by ripening of Ni_3Sn dendrites and growth of Ni(α) phase between the Ni_3Sn arms. If the undercooling before nucleation was below 130 K, bulk melt of the original composition Ni–32.5 wt% Sn existed between the dendrite clusters after recalescence, which then solidified into regular eutectic microstructures. As a result, the structure of the sample consisted of regular eutectic zones and anomalous eutectic zones. If the undercooling before nucleation was above about 130 K, no bulk melts existed after recalescence, so the structures of the samples were completely anomalous eutectic.

1. Introduction

As the undercooling increases, the solidification microstructures of eutectic alloys may change from well-aligned two-phase distribution into an "anomalous eutectic microstructure", which appears to consist of a particulate distribution of one phase distributed in the matrix of another phase. Many studies have reported the formation of such anomalous eutectic microstructures [1–4], but various mechanisms have been proposed, for example; (1) dendritic growth of a solute-rich phase in a partitionless manner followed by intradendritic melting and resolidification [1]; (2) independent simultaneous nucleation and growth of both phases of eutectic [2]; (3) solidification in a non-dendritic fashion and without solute segregation followed by solid-state precipitation of the second phase [3]; (4) formation of a dendritic skeleton of either of the two phases, followed by its segmentation and ripening and the subsequent nucleation of the other phase in the interdendritic liquid regions [4]. In order to obtain a deeper understanding of the solidification mechanisms of undercooled alloys and to confirm the proposed mechanisms, further studies are needed. In the present work, solidification of undercooled eutectic Ni–32.5 wt % Sn alloy was studied, with emphasis on the evolution of the structures and the effect of undercooling on the microstructures.

2. Experimental procedure

The alloys were heated by electromagnetic induction under 4×10^{-3} Pa vacuum. The temperature was measured using an infrared thermometer, and the signal ratios of the infrared thermometer were calibrated against a $PtRh_{30}$–$PtRh_6$ thermocouple. Ni–32.5 wt % Sn alloys were prepared from 99.9% pure nickel and tin.

The alloys were purified to make them undercooled at a slow cooling rate (10–20 K s^{-1}). First, the samples of a weight between 1 and 3 g were superheated cyclically in B_2O_3 slag so that the heterogeneous catalysts were absorbed by the slag, then the samples were cleaned of slag and superheated cyclically at levitation state under vacuum in order to eliminate heterogeneous catalysts by decomposition and evaporation.

3. Results and discussion

3.1. The cooling curve of undercooled Ni–32.5 wt% Sn alloy

The cooling curve is shown schematically in Fig. 1. When the alloy melt was cooled to a temperature T_N, nucleation occurred at one or a few points on the surface of the melt. Subsequently, the solidification interface moved quickly across the melt as the temperature of the sample rose to T_R. This solidification stage may be termed "rapid recalescence". After the rapid recalescence, the crystal grains ripened, and the interdendritic melt continued to solidify as the temperature of the sample rose to T'_R, a temperature usually a little lower than the equilibrium eutectic temperature T_E. This stage may be termed "slow recalescence". After slow recalescence, there was a eutectic solidification

---

* Author to whom all correspondence should be addressed.

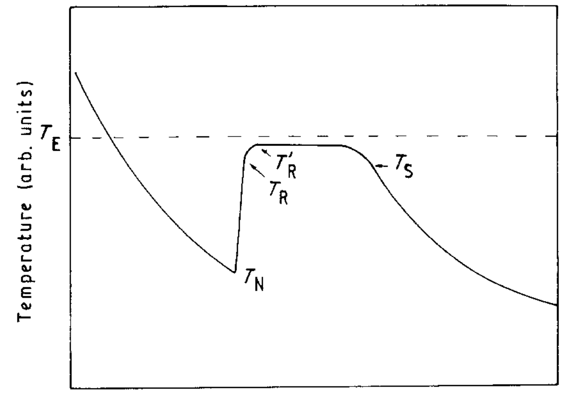

Figure 1 The cooling curve of undercooled Ni–32.5 wt % Sn alloy.

stage, with the temperature keeping nearly constant. In this stage, the temperature at the solidification interface may be near the equilibrium eutectic temperature, but because of the temperature gradient in the sample, the temperature measured by the infrared thermometer is a little lower than the equilibrium eutectic temperature.

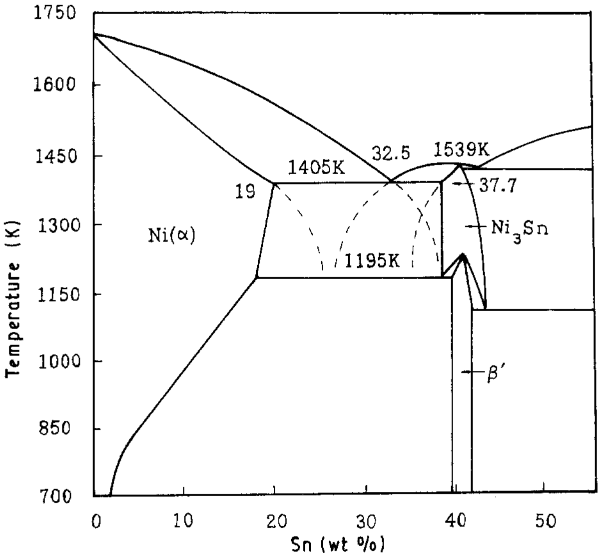

Figure 2 The nickel-rich portion of the Ni–Sn phase diagram.

3.2. Solidification structures

The nickel-rich portion of the Ni–Sn phase diagram is shown in Fig. 2. Solidification of undercooled Ni–32.5 wt % Sn alloy was observed to result in three kinds of microstructures, as shown in Fig. 3. If the undercooling before nucleation was less than about 10 K, the solidification microstructures of the sample are entirely regular eutectic. With increasing undercooling, anomalous eutectic structures appeared, the structures of the sample consist of anomalous eutectic zones and regular eutectic zones. If the undercooling was above about 130 K, the structures of the sample were entirely anomalous eutectic.

At an undercooling range up to 380 K, Ni–32.5 wt % Sn alloy has been observed to solidify into a f c c phase Ni(α) and a hexagonal phase Ni_3Sn, which are the same as the equilibrium phases. Fig. 4 shows the diffraction pattern of a sample solidified from an undercooling of 352 K. Further composition analysis, as shown in Fig. 5, confirmed that the matrix phase (appearing light in the photomicrographs) is Ni_3Sn, and the interdendritic phase is Ni(α) (appearing dark in the photomicrographs). Mass spectrometry analysis shows that the average compositions in the anomalous eutectic zones and that in the regular eutectic zones are both equal to the initial composition Ni–32.5 wt % Sn.

3.3. Solidification mechanism of the undercooled alloys

The alloy melt was cooled in a quartz tube with a nozzle at the bottom. After recalescence, an argon pressure was exerted into the tube to blow off the unsolidified melt through the nozzle; what remained in the tube was the part solidified during recalescence. Fig. 6a shows a cross-section of a sample solidified during recalescence (solidifying from an undercooling of 103 K), where the light zones are crystals, that is, the solidified part during recalescence; the dark zones are holes, namely, the unsolidified part during recalescence. Fig. 6b is an enlarged photograph of Fig. 6a, which shows that the zones solidified during recalescence finally develop into anomalous eutectic microstructures. With increasing undercooling, the amount of melt blown off from the tube after recalescence decreased. When the undercooling was above about 130 K, little melt could be blown off.

It can be seen from Fig. 6a that the crystal grows in a dendritic cluster form during the recalescence stage. After recalescence, the dendritic clusters run through the sample, but bulk melts still exist between the dendritic clusters. With increasing undercooling, the solid fraction formed during recalescence increases, and the volume of the bulk melts between the dendritic clusters decreases. According to the experimental results showing that alloy melt could hardly be blown off from the tube after recalescence if the initial undercooling was above 130 K, it can be deduced that very little bulk melt exists between the dendritic clusters after recalescence if the initial undercooling is above about 130 K.

Because the temperature of the samples rises near the equilibrium eutectic temperature after recalescence, the bulk melts between the dendritic clusters will solidify into regular eutectic microstructures in the eutectic solidification stage, so it can be deduced that the regular eutectic zones in Fig. 3b are formed during the eutectic stage. It can be seen from Fig. 3b that Ni_3Sn phase grows as the leading phase during the recalescence stage. Ni_3Sn phase grows in a dendritic cluster form, forming dendritic skeletons. Ni(α) phase forms between the Ni_3Sn dendritic arms. Ripening of Ni_3Sn dendrites and growth of Ni(α) phase between the Ni_3Sn dendrite arms during and after the recalescence stage lead to the disappearance of the dendritic morphology and the formation of anomalous eutectic microstructures. If the initial undercooling is large enough, no trace of dendritic morphology will remain. The grain sizes of the anomalous

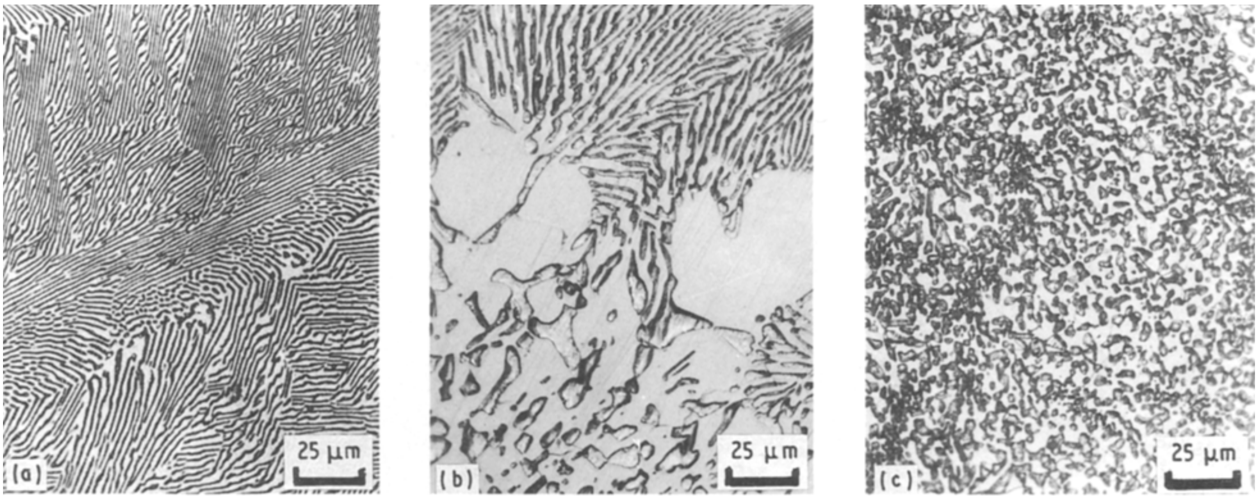

Figure 3 The solidification microstructures of undercooled Ni–32.5 wt % Sn alloy, at ΔT: (a) 10 K, (b) 103 K and (c) 350 K.

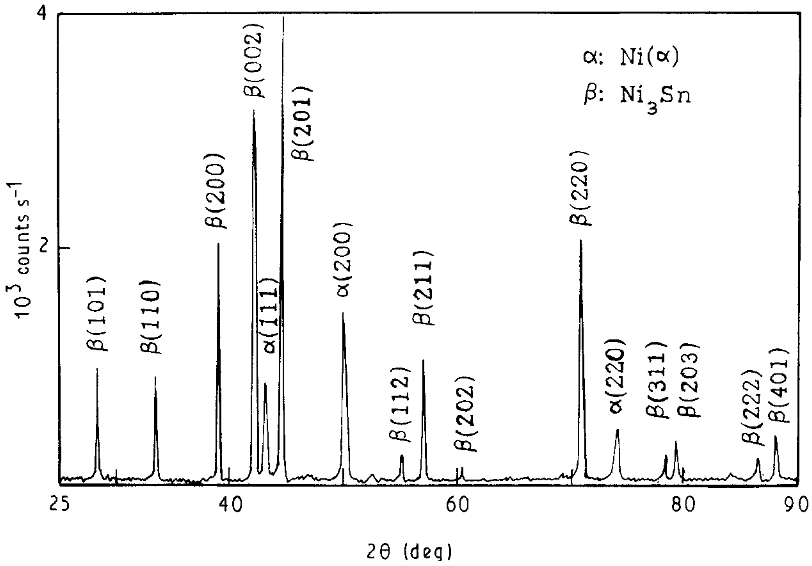

Figure 4 The diffraction pattern of a sample solidified from an undercooling of 352 K.

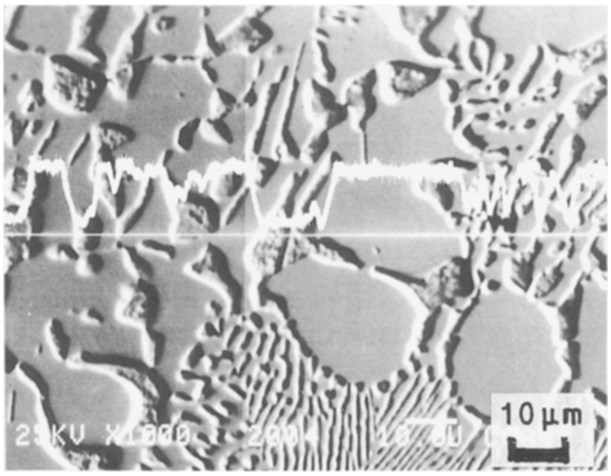

Figure 5 The composition profile of tin in an anomalous eutectic region.

microstructures depend on the initial undercooling of the alloy melt and the local ripening time, which depends on the cooling conditions and the positions in the samples. Generally speaking, large undercooling leads to small dendritic arm spacings and hence results in fine grains. A slow cooling rate leads to a long ripening time and hence results in large grain sizes. For the same reason, the grain sizes increase with the distance radially inwards from the surface in a sample, as is shown in Fig. 7.

3.4. Dendritic growth velocity in undercooled Ni–32.5 wt% Sn alloy

The metastable liquidus and solidus below the eutectic temperature were extrapolated according to the published equilibrium phase diagram and by using a regular solution model [5] to calculate the molar free energies of the liquid phase and Ni(α) solid solution, and using a sublattice model [6] to calculate the molar free energies of Ni$_3$Sn intermetallic compound:

metastable solidus of Ni(α) phase

$$T = 1779 - 3821X_s + 2169X_s^2 \qquad (1)$$

metastable liquidus of Ni(α) phase

$$T = 1843.2 - 2159.7X_L + 298X_L^2 \qquad (2)$$

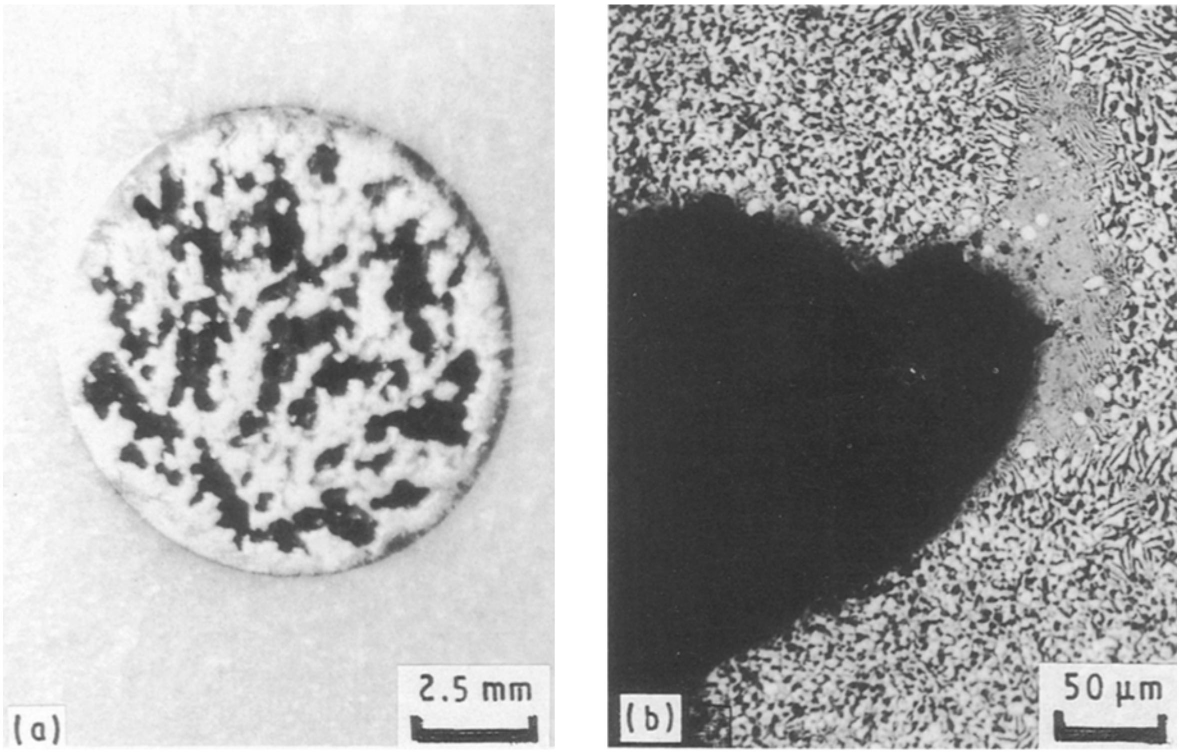

Figure 6 The dendrite clusters formed during recalescence; $\Delta T = 103$ K.

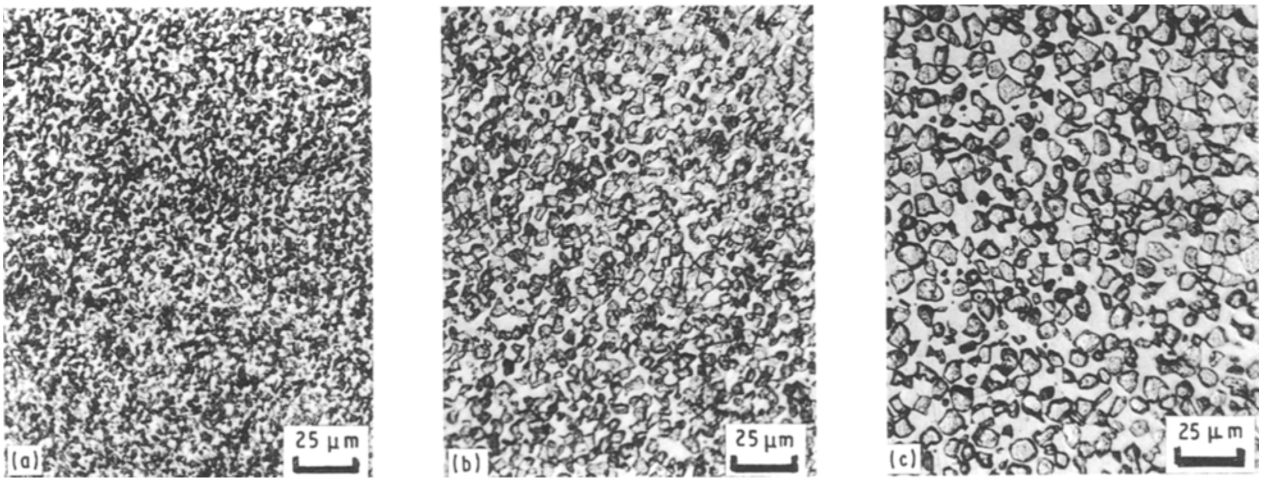

Figure 7 The microstructures of a sample radially inwards from the surface. $\Delta T = 320$ K, distance from the surface: (a) 0, (b) 2.5 mm, (c) 5 mm.

metastable solidus of Ni_3Sn phase

$$T = -2771 + 2.7 \times 10^4 X_s - 4 \times 10^4 X_s^2 \qquad (3)$$

metastable liquidus of Ni_3Sn phase

$$T = 1149 - 299 X_L + 8.1 \times 10^3 X_L^2 \qquad (4)$$

where X_S and X_L are the mole fractions of the tin component in the solid and liquid phases, respectively, T is the temperature in Kelvin.

Using the LKT model [7] and substituting the above equations, the following equations may be obtained

$$\begin{aligned} \Delta T = {} & \frac{\Delta H}{C_p} IV(P_t) + \frac{2\Gamma}{R} + T_L - 1843.2 \\ & + 2159.7 \left[\frac{C_0}{1-(1-K)IV(P_c)} \right] \\ & - 298 \left[\frac{C_0}{1-(1-K)IV(P_c)} \right]^2 \end{aligned} \qquad (5)$$

$$\begin{aligned} K = {} & 0.449 + 0.449 \left[\frac{C_0}{1-(1-K)IV(P_c)} \right] \\ & - 0.062 \left[\frac{C_0}{1-(1-K)IV(P_c)} \right]^2 \\ & + 4.16 \times 10^{-4} \frac{\Gamma}{R} \end{aligned} \qquad (6)$$

$$R = \frac{\dfrac{\Gamma}{\sigma^*}}{\left[\dfrac{P_t \Delta H}{C_p}(1-n) - \dfrac{2 m_c P_c C_o (K-1)}{1-(1-K)IV(P_C)}(1+g) \right]} \qquad (7)$$

where

$$n = \frac{1}{(1 + 1/\sigma^* P_t^2)^{1/2}}$$

$$P_t = \frac{VR}{2\alpha}$$

$$g = \frac{2K}{1 - 2K - (1 + 1/\sigma^* P_t^2)^{1/2}}$$

$$P_c = \frac{VR}{2D}$$

ΔH is the latent heat of fusion, C_p is the specific heat of the liquid alloy, R is the dendrite tip radius, V is the dendrite tip velocity, D is the solute interdiffusion coefficient in the liquid, α is the thermal diffusivity, σ^* is the stability constant of a value about 0.025, K is the partition ratio of the tin component between the solid phase and the liquid phase, $\mathrm{IV}(P)$ is the Ivantsov function, m_L is the liquidus slope.

For a given ΔT, according to Equations 5–7 and the parameters listed in Table I, the dendrite tip velocity may be calculated, as shown in Fig. 8. It can be seen from Fig. 8 that the dendrite tip velocity of Ni_3Sn phase is greater than that of Ni(α) phase for a given undercooling. Therefore, when the undercooled eutectic Ni–32.5 wt % Sn alloy solidifies, Ni(α) phase and Ni_3Sn phase cannot grow in a matching form, to produce aligned two-phase distribution microstructures, but Ni_3Sn phase grows as the leading phase, to form Ni_3Sn dendritic skeletons.

TABLE I The parameters used in calculating the dendrite tip velocity [8, 9]

C_p	$500\ \mathrm{J\,kg^{-1}\,K^{-1}}$
ΔH [Ni(α)]	$1.5 \times 10^5\ \mathrm{J\,kg^{-1}}$
ΔH [Ni_3Sn]	$2.04 \times 10^5\ \mathrm{J\,kg^{-1}}$
Γ [Ni(α)]	$2.98 \times 10^{-7}\ \mathrm{Km}$
Γ [Ni_3Sn]	$2.1 \times 10^{-7}\ \mathrm{Km}$
ρ	$8400\ \mathrm{kg\,m^{-3}}$
α	$5 \times 10^{-6}\ \mathrm{m^2\,s^{-1}}$
D [Sn]	$5 \times 10^{-9}\ \mathrm{m^2\,s^{-1}}$
C_o	0.1923 mol
T_L	1405 K

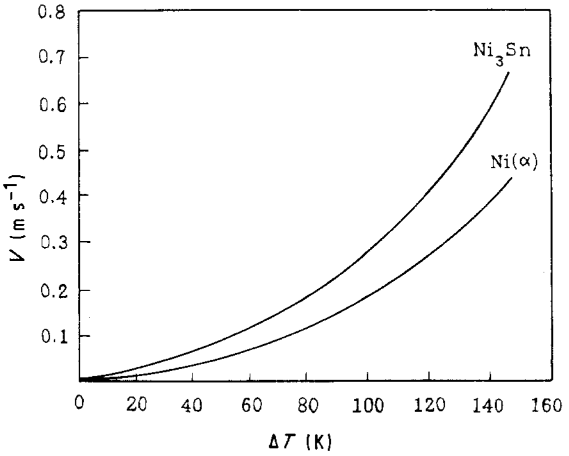

Figure 8 The dendrite tip velocity versus undercoolings for Ni–32.5 wt % Sn alloy.

4. Conclusions

1. When undercooled eutectic Ni–32.5 wt % Sn alloy recalesces, Ni(α) phase and Ni_3Sn phase do not grow in a matching form to produce regular eutectic microstructures, but Ni_3Sn phase grows as the leading phase to form a Ni_3Sn dendritic skeleton, and an Ni(α) phase forms between the Ni_3Sn dendrite arms, because the dendrite tip velocity of Ni_3Sn is greater than that of Ni(α) in undercooled Ni–32.5 wt % Sn melt.
2. Undercooled Ni–32.5 wt % Sn alloy solidifies into dendritic clusters during recalescence, which subsequently develop into anomalous eutectic microstructures by Ni_3Sn dendrite ripening and growth of the interdendritic Ni(α) phase.
3. If the initial undercooling is below about 10 K, Ni–32.5 wt % Sn alloy solidifies into regular eutectic structures. If the initial undercooling is between 10 K and about 130 K, bulk melts of the initial composition still exist between the dendritic clusters after recalescence, and the bulk melts solidify into regular eutectic microstructures in the following eutectic stage, so the structures in the sample consist of anomalous eutectic zones and regular eutectic zones. If the initial undercooling is above about 130 K, no bulk melts exist after recalescence, so the microstructures in the sample are completely anomalous eutectic.

References

1. T. Z. KATTAMIS and M. C. FLEMINGS, *Metall. Trans.* **1A** (1970) 1449.
2. G. J. ABBASCHIAN and M. C. FLEMINGS, *ibid.* **14A** (1983) 1147.
3. M. G. CHU, Y. SHIONARA and M. C. FLEMINGS, *ibid.* **15A** (1984) 1303.
4. S. N. TEWARI, *ibid.* **18A** (1987) 525.
5. S. HASSAM, *ibid.* **19A** (1988) 409.
6. J. L. MURRAY, *ibid.* **19A** (1988) 243.
7. R. TRIVEDI and W. KURZ, *Acta Metall.* **34** (1986) 1663.
8. Y. WU, T. J. PILLONE, Y. SHIOHARA, *Metall. Trans.* **18A** (1987) 915.
9. C. J. SMITHELLS, “Metals Reference Book”, 5th Edn. (Butterworth, London, 1976) p. 186.

Received 4 November 1991
and accepted 14 August 1992